

# Reconfigurable directional couplers and junctions optically induced by nondiffracting Bessel beams

Zhiyong Xu, Yaroslav V. Kartashov, and Lluís Torner

*ICFO–Institut de Ciències Fotoniques, and Department of Signal Theory and Communications, Universitat Politècnica de Catalunya, 08034 Barcelona, Spain*

Victor A. Vysloukh

*Departamento de Física y Matemáticas, Universidad de las Américas–Puebla, Santa Catarina Martir, 72820, Puebla, Mexico*

Received November 1, 2004

We put forward the concept of reconfigurable structures optically induced by mutually incoherent nondiffracting Bessel beams in Kerr-type nonlinear media. We address collinear couplers and X junctions and show how one can tune the switching properties of such structures by varying the intensity of the Bessel beams. © 2005 Optical Society of America

*OCIS codes:* 190.5530, 190.4360, 060.1810.

Since its theoretical prediction<sup>1</sup> and experimental observation,<sup>2,3</sup> guiding of probe beams by bright and dark spatial solitons has been studied comprehensively because of its potential applications to all-optical switching. The canonical example is a nonlinear directional coupler that consists of several parallel soliton-induced waveguides,<sup>4,5</sup> for which an input signal periodically switches between the output channels.<sup>6–9</sup> Another important example is the X junction formed by several intersecting soliton beams.<sup>10,11</sup> The potential of such structures relies on the possibility of tuning the device characteristics by changing the properties of the solitons employed to produce the switching structure. Here we suggest a different way to create reconfigurable devices for all-optical switching, based on the concept of optical lattices.

It was demonstrated recently<sup>12–14</sup> that reconfigurable honeycomb optical lattices can be produced by several interfering plane waves propagating in a linear regime, whereas vectorial interactions in slow Kerr-type media can be used to guide soliton beams in the lattice. Lattices with a radial symmetry induced by nondiffracting Bessel beams are also possible and furnish a wealth of new opportunities.<sup>15–18</sup> For example, the nondiffracting beams can induce well-defined guiding channels that can trap and steer soliton beams. Good approximations of Bessel beams can be generated experimentally.<sup>19</sup> Here we address directional couplers and X junctions induced by several mutually incoherent parallel or intersecting Bessel beams and show the various soliton-switching schemes accessible with such optically induced and, hence, tunable devices. Notice that, in contrast to Refs. 4 and 5, which address the switching of linear beams in soliton-induced waveguides, here we show that guiding structures created with linear beams lead to soliton control.

We consider the propagation of a light beam along the  $z$  axis in a nonlinear cubic Kerr-type medium

with an optically induced modulation of the refractive index. The evolution of the complex amplitude  $q$  of the field can be described by the equation

$$i \frac{\partial q}{\partial \xi} = -\frac{1}{2} \left( \frac{\partial^2 q}{\partial \eta^2} + \frac{\partial^2 q}{\partial \zeta^2} \right) - q|q|^2 - pR(\eta, \zeta, \xi)q, \quad (1)$$

where  $\eta$ ,  $\zeta$ , and  $\xi$  stand for the transverse and the longitudinal coordinates scaled to the beam width and the diffraction length, respectively. We assume that the refractive-index modulation is induced by several incoherent zero-order Bessel beams, so the refractive-index profile features the total intensity of the beams. Parameter  $p$  is proportional to the modulation depth, and in the simplest case of two incoherent Bessel beams the refractive-index modulation is described by

$$R(\eta, \zeta, \xi) = J_0^2 \{ (2b_{\text{lin}})^{1/2} [(\eta + \eta_0 - \alpha\xi)^2 + \zeta^2]^{1/2} \} \\ + J_0^2 \{ (2b_{\text{lin}})^{1/2} [(\eta - \eta_0 + \alpha\xi)^2 + \zeta^2]^{1/2} \}.$$

Scaling parameter  $b_{\text{lin}}$  defines the radii of the rings of Bessel beams, and we take it small enough to ensure that the width of the central beam core ( $20 \mu\text{m}$ ) greatly exceeds the wavelength,  $2\eta_0$  is the initial separation between beam centers, and  $\alpha$  defines the head-on intersection angle. Equation (1) admits of several conserved quantities, including the power or energy flow,  $U = \int_{-\infty}^{\infty} \int_{-\infty}^{\infty} |q|^2 d\eta d\zeta$ . We study the propagation of ground-state solitons launched parallel to one of the guiding channels of the structure. When searching for input soliton profiles we assume that only one guiding channel is present. The soliton profile has the form  $q(\eta, \zeta, \xi) = w(\eta, \zeta) \exp(ib\xi)$ , where  $w(\eta, \zeta)$  is a real function and  $b$  is a real propagation constant. As  $b \rightarrow \infty$  the soliton width goes to zero, while its power approaches the critical value  $U_{\text{cr}} \approx 5.85$  given by the power of an unstable soliton in a uniform cubic medium. Here we consider solitons

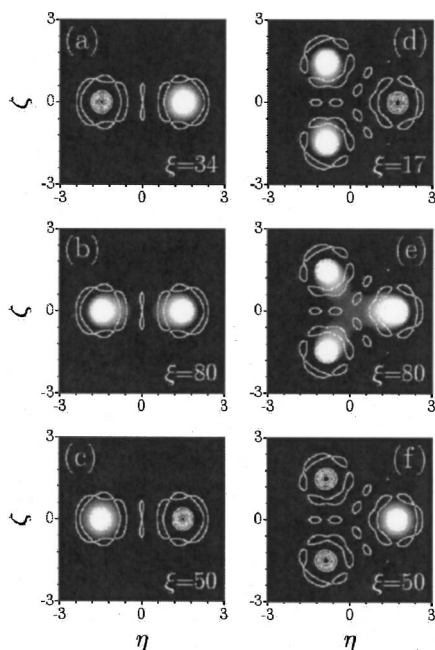


Fig. 1. Switching in (a)–(c) two- and (d)–(f) three-core optically induced couplers. Output intensity distributions are shown at  $\xi \approx L_c$ . White contour curves are aids to the eye and show the positions of optically induced channels. In the two-core coupler the soliton was launched into the left-hand channel; in the three-core coupler it was launched into the right-hand channel. Input power (a)  $U=1.56$ , (b) 1.67, (c) 3.1, (d) 1.56, (e) 2.15, and (f) 2.68. Parameters:  $p=5$ ,  $2\eta_0=3$ ,  $b_{\text{lin}}=10$ .

with powers well below the critical one, when coupling between Bessel waveguides is considerable. In the case of X junctions we impose phase tilt  $\exp(i\alpha\eta)$  on the input solitons. Our primary aim in this Letter is to study the effect of modulation depth  $p$ , intersection angle  $\alpha$ , and input soliton power  $U$  on possible switching scenarios.

First, we address the properties of reconfigurable directional couplers induced with collinear incoherent Bessel beams ( $\alpha=0$ ). Because of the overlap of the soliton tails guided by neighboring Bessel channels, energy is exchanged periodically between the channels on propagation. The rate of the energy exchange is given by the overlap integral, which increases with a decrease of separation between waveguides or with an increase of refractive-index modulation depth.

Figure 1 shows different soliton switching scenarios in two-core [Figs. 1(a)–1(c)] and three-core [Figs. 1(d)–1(f)] couplers for different input powers. At small powers one achieves almost total energy transfer from the input guiding channel into neighboring channels at coupling length  $\xi=L_c$  [Figs. 1(a) and 1(d)]. Note that in a three-core coupler the energy is equally redistributed between two output channels. Similar phenomena occur with more-complicated Bessel beam arrays arranged in ring configurations when the energy flow of a soliton launched into a single channel is redistributed among all other channels at the output. Because of the periodic character of the energy exchange the input field distribution is completely restored at  $\xi=2L_c$ . At the critical power level, the energy is

equally distributed among all channels of the coupler [Figs. 1(b) and 1(e)]. In this case, coupling length  $L_c$  diverges. Finally, at high powers there is no energy transfer into neighboring channels [Figs. 1(c) and 1(f)]. Thus the optically induced coupler behaves as the sought-after nonlinear directional coupler.

The variation of the coupling length and the normalized transmission efficiency versus the input power for a two-core coupler are shown in Figs. 2(a) and 2(b), respectively. The transmission efficiency is defined as the ratio of energy concentrated in the output channel to that concentrated in the input channel. The coupling length increases and the transmission efficiency decreases as the input power approaches the critical value corresponding to equal energy distribution in all channels. To stress the reconfigurability afforded by optically induced couplers, in Figs. 2(c) and 2(d) we plot the coupling length and the transmission efficiency, respectively, versus the modulation depth  $p$  at fixed input power. The modulation depth can be directly controlled by intensities of Bessel beams forming the coupler. Because at fixed power the soliton supported by a single channel becomes narrower with increasing  $p$ , the transmission efficiency decreases above the critical modulation depth, and all switching conditions from total to negligible energy transfer can be achieved.

Second, we address properties of X junctions created with two intersecting Bessel beams ( $\alpha \neq 0$ ). The initial separation between guiding channels is high enough that, at the initial stage of propagation, a soliton launched into the right-hand channel of the junction is almost unaffected by the presence of the left-hand channel. We calculate the transmission efficiency, defined as the ratio of output power concentrated in the central core of the left channel at  $\xi=2\eta_0/\alpha$  to the input power concentrated in the central core of the right channel at  $\xi=0$ . Figure 3(a) shows that the intersection of two incoherent Bessel beams produces an area of locally increased refractive index that is elongated along the  $\xi$  axis. The

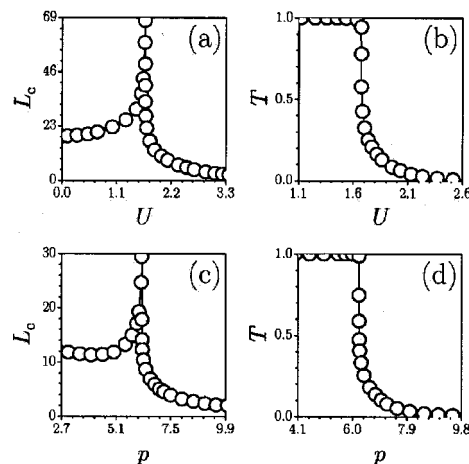


Fig. 2. (a) Coupling length and (b) normalized transmission efficiency versus input power at  $p=5$  and  $\eta_0=1.5$ . (c) Coupling length and (d) normalized transmission efficiency versus modulation depth at  $U=2$  and  $\eta_0=1$ . In both cases  $b_{\text{lin}}=10$ .

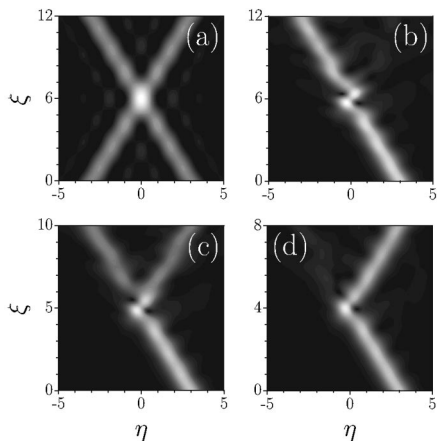


Fig. 3. (a) X junction made by intersecting incoherent Bessel beams at  $\alpha=0.5$ . Different soliton propagation scenarios at (b)  $\alpha=0.5$ , (c)  $\alpha=0.6$ , and (d)  $\alpha=0.75$  are shown. Intensity distributions are shown at  $\zeta=0$ . In all cases  $p=5$ ,  $U=2$ ,  $2\eta_0=6$ , and  $b_{\text{lin}}=2$ .

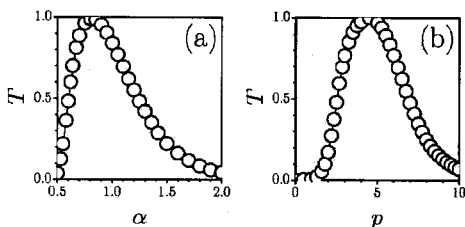


Fig. 4. (a) Normalized transmission efficiency versus intersection angle at  $p=5$  and  $U=2$ . (b) Normalized transmission efficiency versus modulation depth at  $\alpha=0.75$  and  $U=2$ . Parameters:  $2\eta_0=6$  and  $b_{\text{lin}}=2$ .

smaller the intersection angle, the longer the area of locally increased refractive index. When the soliton from the right-hand channel enters this area it is bounced back, as one can see from Figs. 3(b)–3(d). Depending on the intersection angle (i.e., the length of the intersection area), the soliton remains in the input channel [Fig. 3(b)], splits into two beams [Fig. 3(c)], or experiences total switching into the left-hand channel [Fig. 3(d)]. The potential applications of this effect for angle-controlled soliton switching are clearly visible. The normalized transmission efficiency versus intersection angle is shown in Fig. 4(a). Almost 100% switching contrast can be achieved in such an X junction. With further growth of  $\alpha$  the transmission efficiency decreases monotonically. Small angles are not shown in Fig. 4(a) because in this case small modifications of the input angle result in drastic changes in switching dynamics and fast oscillations of the curve  $T(\alpha)$  at  $\alpha \rightarrow 0$ . We found that switching with high contrast can be achieved by tuning the depth of refractive-index modulation  $p$  [Fig. 4(b)]. There exists an optimal value of  $p$  that yields

almost total soliton switching into the left-hand channel at fixed input power and intersection angle. This is another confirmation of the potential of reconfigurable guiding structures induced with arrays of Bessel beams for all-optical soliton control.

In conclusion, we have shown that reconfigurable directional couplers and X junctions induced with nondiffracting Bessel beams afford a variety of opportunities for soliton switching. The key feature that we have put forward is the possibility of controlling the device dynamics by adjusting the properties of the Bessel beams that are used to induce the coupler.

This work has been partially supported by the government of Spain through grant BFM2001-2861 and the Ramon-y-Cajal program.

Y. V. Kartashov's e-mail address is Yaroslav.Kartashov@icfo.es.

## References

1. A. W. Snyder, D. J. Mitchell, L. Poladian, and F. Ladouceur, *Opt. Lett.* **16**, 21 (1991).
2. R. De La Fuente, A. Barthelemy, and C. Froehly, *Opt. Lett.* **16**, 793 (1991).
3. B. Luther-Davies and Y. Xiaoping, *Opt. Lett.* **17**, 496 (1992).
4. S. Lan, E. DelRe, Z. Chen, M. Shih, and M. Segev, *Opt. Lett.* **24**, 475 (1999).
5. E. DelRe, B. Crosignani, P. Di Porto, E. Palange, and A. J. Agranat, *Opt. Lett.* **27**, 2188 (2002).
6. M. Morin, G. Duree, G. Salamo, and M. Segev, *Opt. Lett.* **20**, 2066 (1995).
7. M. Shih, M. Segev, and G. Salamo, *Opt. Lett.* **21**, 931 (1996).
8. M. Shih, Z. Chen, M. Mitchell, M. Segev, H. Lee, R. S. Feigelson, and J. P. Wilde, *J. Opt. Soc. Am. B* **14**, 3091 (1997).
9. V. Aleshkevich, Y. V. Kartashov, and V. A. Vysloukh, *Opt. Commun.* **192**, 365 (2001).
10. G. E. Torres-Cisneros, J. J. Sánchez-Mondragón, and V. A. Vysloukh, *Opt. Lett.* **18**, 1299 (1993).
11. A. Guo, M. Henry, G. J. Salamo, M. Segev, and G. L. Wood, *Opt. Lett.* **26**, 1274 (2001).
12. J. W. Fleischer, M. Segev, N. K. Efremidis, and D. N. Christodoulides, *Nature (London)* **422**, 147 (2003).
13. D. Neshev, E. Ostrovskaya, Y. Kivshar, and W. Krolikowski, *Opt. Lett.* **28**, 710 (2003).
14. H. Martin, E. D. Eugeniya, Z. Chen, and D. N. Christodoulides, *Phys. Rev. Lett.* **92**, 123902 (2004).
15. Y. V. Kartashov, V. A. Vysloukh, and L. Torner, *Phys. Rev. Lett.* **93**, 093904 (2004).
16. Y. V. Kartashov, A. A. Egorov, V. A. Vysloukh, and L. Torner, *J. Opt. B: Quantum Semiclassical Opt.* **6**, 444 (2004).
17. Y. V. Kartashov, A. A. Egorov, V. A. Vysloukh, and L. Torner, *Phys. Rev. E* **70**, 065602(R) (2004).
18. Y. V. Kartashov, V. A. Vysloukh, and L. Torner, *Phys. Rev. Lett.* **94**, 043902 (2005).
19. V. Kettunen and J. Turunen, *Opt. Lett.* **23**, 1247 (1998).